Locations of Landau Singularities*

RICHARD E. NORTON
Department of Physics, University of California, Los Angeles, California
(Received 23 April 1964)

It is shown for the third-order triangle and the fourth-order box Feynman diagrams that singularities exist on the physical boundaries of the amplitudes if, and only if, the external momenta are such as to allow the reactions to actually proceed with real intermediate particles. If, furthermore, the information concerning the locations and appropriate branches of singularities implied by this principle is combined with the requirement that discontinuities be given by Cutkosky's rules, the amplitudes are uniquely determined.

I. INTRODUCTION

An essential difficulty which has thwarted attempts to construct schemes for the calculation of arbitrary S-matrix elements is that there appear large numbers of singularities dispersed in an unknown fashion on the many Riemann sheets of the transition amplitudes. Although equations for singularity surfaces[1] and expressions for residues and discontinuities[2] can be obtained, no comparable methods exist which may be employed to determine on which Riemann sheets the singularities are located. This lack implies that the functions which describe the residues and discontinuities are ambiguous in that the proper branches for these expressions are not determined.

In this paper the singularities characteristic of the triangle and box Feynman-Cutkosky diagrams (Figs. 1 and 5) are studied with an eye toward obtaining results which appear general enough to shed light on this problem. Particular attention is devoted to understanding the physical processes with which singularities correspond; the motivation for this effort is the hope that sufficient insight will be gained to help clarify the situation which is so complicated from a mathematical point of view. The results of this work have as yet only been verified for the two diagrams mentioned. Nevertheless, many features will appear readily generalizable.

Every diagram, for example the triangle in Fig. 1, will appear internally in an infinite number of S-matrix amplitudes. One can connect an arbitrary number (within limits imposed by the conservation laws) of incoming and outgoing particles at each of the external vertices. Viewed this way, a given graph has an extensive range of its external variables where it contributes to physical processes. For example, the graph in Fig. 1 is physical if $M_i^2 \geq (M_j+M_k)^2$, or if $M_i^2 \leq (M_j-M_k)^2$. That is, it can contribute to some physical amplitudes whenever

$$\Delta(M_1^2,M_2^2,M_3^2) \equiv M_1^4+M_2^4+M_3^4-2M_1^2M_2^2 -2M_1^2M_3^2-2M_2^2M_3^2 \geq 0, \quad (1)$$

and all the M_i^2 are real.

Suppose that it is possible to connect particles to the external vertices of a diagram with momenta such that the transition thereby represented can actually occur with some, or all, of the internal particles propagating freely—on the mass shell with real, future timelike momenta. For values of the external variables which satisfy these requirements, the diagram has a Landau singularity residing on the physical boundary[3] of the complex amplitude.[4] Further, no singularity ever lies on the physical boundary unless it corresponds in this way to a transition involving real intermediate particles.[5]

The first object of this paper is to verify that these statements are true for the two amplitudes of Figs. 1 and 5. Secondly, we want to point out that these amplitudes are unambiguously determined once the consequences of these remarks are supplemented by Cutkosky's[2] rules for the calculation of discontinuities. This result follows despite the fact that not all the singularities refer to possible transitions with real intermediate particles. The existence of such singularities arise from the form of the mathematical expressions for the discontinuities, and their proper Riemann sheets are fixed by requiring that there is no process for which they reside on the physical boundary.

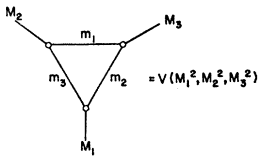

FIG. 1. The triangle diagram.

* Supported in part by the National Science Foundation.

[1] L. D. Landau, Nucl. Phys. **13**, 181 (1959); P. V. Landshoff, J. C. Polkinghorne, and J. E. Taylor, Nuovo Cimento **19**, 939 (1961); R. J. Eden, Phys. Rev. **121**, 1567 (1961).

[2] R. E. Cutkosky, J. Math. Phys. **1**, 429 (1960); Phys. Rev. Letters **4**, 624 (1960).

[3] In contrast to the position of the so-called anomalous threshold [R. Karplus, C. M. Sommerfield, and E. M. Wichman, Phys. Rev. **111**, 1187 (1958); **114**, 375 (1959); S. Mandelstam, Phys. Rev. Letters **4**, 84 (1960)] which is never in the physical range of variables for amplitudes with two stable, initial particles. It may, however, get close: P. V. Landshoff and S. B. Treiman, Phys. Rev. **127**, 649 (1962); P. V. Landshoff, Phys. Letters **3**, 116 (1962). R. Aaron, Phys. Rev. Letters **10**, 32 (1963); also Ref. 10.

[4] L. S. Liu, Phys. Rev. **125**, 761 (1962); R. E. Cutkosky, Rev. Mod. Phys. **33**, 448 (1961).

[5] Subsequent to this work, we have been able to show the equivalence between this condition for a physical interpretation and the usual one of positiveness of the Feynman parameters. See forthcoming paper by S. Coleman and R. E. Norton.

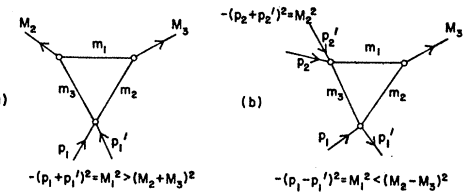

FIG. 2. Examples of two processes for which the point $x_1=M_1^2=(m_2+m_3)^2$ can fall in the physical region. For case (a), $(M_2+M_3)^2>(m_2+m_3)^2$; for (b), $(m_2+m_3)^2<(M_2-M_3)^2$.

Section II is devoted to a study of the triangle diagram. The physical "pictures" of the singularities are discussed, and from these considerations the values of the external variables are obtained which locate singularities on the physical boundary. It is then shown that these essentially kinematic conditions, together with generalized unitarity,[2] suffice to determine the amplitude. In Sec. III the corresponding steps are carried out for the box diagram in Fig. 5. The results concerning the location of singularities are also shown to agree with those obtained by analytically continuing in the external masses.[6] Finally, in Sec. IV, we summarize our results and make some brief general remarks.

II. THE TRIANGLE DIAGRAM

We study the diagram of Fig. 1, choosing for convenience all particles to be spinless. Employing the notation $s_i=M_i^2$, the analytic properties of the triangle graph $V(s_1,s_2,s_3)$ can be displayed, for example, in the variable s_1, by the dispersion relation[7]

$$V(s_1,s_2,s_3)=\frac{1}{\pi}\int_{(m_2+m_3)^2}^{\infty}\frac{ds_1'}{s_1'-s_1}V_1(s_1',s_2,s_3)\,, \quad (2)$$

where

$$V_1(s_1,s_2,s_3)=\Delta^{-1/2}(s_1,s_2,s_3)\,\ln[\alpha_1+\beta/\alpha_1-\beta]\,, \quad (3)$$

$$\alpha_1=s_1^2-s_1(m_1^2+m_2^2+m_3^2+s_2+s_3)+(m_2^2-m_3^2)(s_2+s_3)\,, \quad (4)$$

$$\beta=\Delta^{1/2}(s_1,m_2^2,m_3^2)\Delta^{1/2}(s_1,s_2,s_3)\,, \quad (5)$$

and Δ is defined in Eq. (1). Sufficient conditions for the validity of Eq. (2) can be expressed simply in terms of the variables x_i,[8] defined by

$$x_i=(s_i-m_j^2-m_k^2)/2m_jm_k \quad (i,j,k \text{ different}). \quad (6)$$

These conditions are fulfilled if $x_2+x_3<0$, $x_2<1$, and $x_3<1$. In the discussion it is often useful to replace the dependence upon the s_i by the x_i. Both variables will be used interchangeably. For $x_i>1$, the vertex "i" is externally unstable, $M_i^2>(m_j+m_k)^2$; for $x_i<-1$, it is internally unstable in the sense that $m_j^2>(M_i+m_k)^2$ or $m_k^2>(M_i+m_j)^2$.

We must consider the following Landau singularities which occur in V:[7]

(1) the normal thresholds

$$s_i=(m_j+m_k)^2, \quad \text{or} \quad x_i=1\,, \quad (7a)$$

(2) the "abnormal" thresholds

$$s_i=(m_j-m_k)^2, \quad \text{or} \quad x_i=-1\,, \quad (7b)$$

(3) the triangle singularities[9]

$$x_i=L_{jk}^{\pm}\,, \quad (7c)$$

with

$$L_{jk}^{\pm}\equiv -x_jx_k\pm[(1-x_j^2)(1-x_k^2)]^{1/2}. \quad (8)$$

The amplitude in Fig. 1 also has a non-Landauian singularity[2,10] given by $\Delta(s_1,s_2,s_3)=0$. This feature is discussed at the end of this section.

Let us first discuss the normal threshold singularities in Eq. (7a). In terms of s_1 the normal threshold is manifest in Eq. (2). As mentioned in Sec. I, whenever $(m_j+m_k)^2>(M_j+M_k)^2$ or $(m_j+m_k)^2<(M_j-M_k)^2$, the point $s_i=(m_j+m_k)^2$ lies in the physical region of s_i. Examples of both possibilities are shown in Fig. 2. We now ask the question—when $s_i=(m_j+m_k)^2$ is in the physical region, can the particles with masses m_j and m_k actually be created and propagate for an arbitrarily long time before making the final steps of the transition? The answer is obviously yes. When $s_i=(m_j+m_k)^2$ the relative velocity of m_j and m_k is zero—they do not move apart—and there is no geometrical reason why they can't take as long as they please to produce the final state. We conclude that the normal thresholds are always on the physical boundary.

The abnormal thresholds in Eq. (7b) can be thought of as referring to the situation where only two particles propagate on the mass shell; the first existing for an arbitrarily long time and then interacting at a vertex to produce the next one with the same velocity. If this could occur, it would be necessary that the part of the amplitude which connects the creation of the first particle to the destruction of the second exists for the

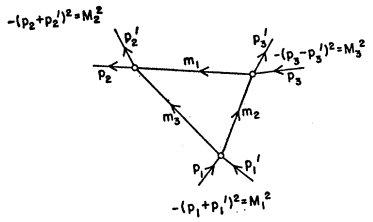

FIG. 3. An example of a process which can occur with all three internal particles propagating freely.

[6] See, for example, S. Mandelstam, Phys. Rev. **112**, 1344 (1958); C. Fronsdal, R. E. Norton, and K. T. Mahanthappa, J. Math. Phys. **4**, 859 (1963); Francis R. Halpern, *ibid.* **4**, 879 (1963).

[7] C. Fronsdal and R. E. Norton, J. Math. Phys. **5**, 100 (1964); G. Bonnevay, I. J. R. Aitchison, and J. S. Dowker, Nuovo Cimento **21**, 1001 (1961).

[8] J. Tarski, J. Math. Phys. **1**, 429 (1960).

[9] We define L_{jk}^{+} to have the positive square root when $-1<x_j<1$ and $-1<x_k<1$. The $L_{jk}^{\pm}$ are then determined at all other values of x_j and x_k providing we don't cross the lines $|x_j|>1$ and $|x_k|>1$.

[10] D. B. Fairlie, P. V. Landshoff, J. Nuttall, and J. C. Polkinghorne, J. Math. Phys. **3**, 594 (1962).

total time both particles are present. However, this would require at least one more real internal particle to propagate this part of the interaction. We conclude that the abnormal thresholds are never on the physical boundary.

The singularities in Eq. (7c) occur because at these points the argument of the logarithm in Eq. (3) has a factor which vanishes (or diverges); $\alpha_1^2-\beta^2\sim(x_iL_{jk}^-)\times(x_i-L_{jk}^+)$. Their existence reflects the possibility that all three intermediate particles can be on the mass shell. An example is shown in Fig. 3.[11] In this case $s_1>(m_2+m_3)^2$, $s_2>(m_1+m_3)^2$, and $s_3<(m_1-m_2)^2$. Equivalently, $x_1>1$, $x_2>1$, and $x_3<-1$. If x_1 and x_2 are held fixed, and the value of x_3 sought which allows the process of Fig. 3, we obtain $x_3=L_{12}^+$. Conversely, if x_3 and $x_2(x_1)$ are fixed, the required value of $x_1(x_2)$ is $L_{23}^-(L_{13}^-)$.

It is clear that, except for variations obtained by relabeling the vertices, the process in Fig. 3 is the only one that can actually occur with three real intermediate particles. The kinematic and geometric requirements which allow this process (and the ones equivalent to it) should therefore be the necessary and sufficient conditions for a triangle singularity to be located on the physical boundary of an amplitude. That these conclusions are valid for the diagram of Fig. 1 can readily be verified by comparing them with the positions of the $L_{ij}^{\pm}$ as determined by analytically continuing $V(s_1,s_2,s_3)$ in the s_i. Since the latter results are reasonable well known and available in the literature,[7,11] we do not discuss them further here.

We now want to show all the singularities of the third-order vertex graph are located by combining our kinematical considerations with Cutkosky's rules. One simple way to accomplish this is to adjust x_2 and x_3 so that for some value of $x_1>1$ the process of Fig. 3 can occur. We therefore fix $x_2>1$, $x_3<-1$, and $x_2+x_3<0$. The triangle singularities $L_{23}^{\pm}$ then lie along the positive x_1 axis as shown in Fig. 4. We are aware of only the three singularities, $x_1=1$, $x_1=L_{23}^+$, and $x_1=L_{23}^-$, and we know that just the first two lie on the physical boundary. Since L_{23}^+ resides at a physically accessible value of s_1 (if $M_3^2<0$, the real s_1 axis is completely accessible) and does not, for these values of x_2 and x_3, correspond to a realizable process with

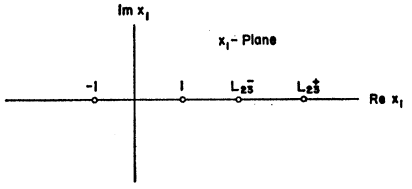

FIG. 4. The positions of the triangle singularities in the x_1 plane when $x_2>1$ and $x_3<-1$.

[11] The considerations here resemble those by I. J. R. Aitchison, Phys. Rev. **133**, B1257 (1964).

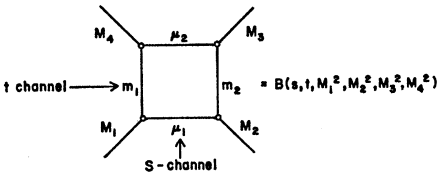

FIG. 5. The box diagram.

real intermediate particles, it is not on the physical boundary.

Let us now employ Cutkosky's rules to calculate the discontinuity across the branch cut from $x_1=1$. We run this cut along the positive real axis, for example, and construct the dispersion integral which expresses this contribution to the amplitude. If the discontinuity, itself, has any singularities for $x_1>1$ (in this case at L_{23}^+ and L_{23}^-), we run the cut under these singularities so that the part of the amplitude thus far constructed has only the singularity $x_1=1$ on the physical boundary. That is, we don't want the singularity of $(x_1'-x_1)^{-1}$ to "pinch"[1] the contour against these other singularities when x_1 approaches the cut from above. Next we repeat the process and construct the dispersion integral contributed by the cut from L_{23}^-. The resulting two expressions can then be combined to yield one dispersion integral whose contour runs from $+1$ to ∞ over L_{23}^- and under L_{23}^+.[7]

The formula for $V(s_1,s_2,s_3)$ obtained in this manner agrees essentially with Eq. (2) when the latter is continued to $x_2>1$ and $x_3<-1$. There is, however, still an ambiguity in that we haven't determined the proper branch of the logarithm in Eq. (3). We decide this point by noticing that on all but the principal branch of the logarithm, the zeros of Δ in Eq. (3) are singular. These zeros occur at $s_1=(M_2\pm M_3)^2$ and are the end points of the physical values of s_1 when they lie on the real axis. It follows that if either of them is located on the real axis, on the unphysical side of the cut (so as to pinch against x), it must do so when the logarithm assumes its principal value. This requirement implies a unique branch of the logarithm.

III. THE BOX DIAGRAM

In this section, we study the diagram of Fig. 5. We apply to it the program outlined in Sec. I and discussed in detail for the triangle graph in Sec. II. We first find the kinematic conditions which locate singularities on the physical boundary, and then show that the conclusions of this effort agree with those obtained by analytic continuation of the box diagram amplitude. Finally, we argue that the amplitude is determined once these results are combined with Cutkosky's rules.

A. Kinematical Considerations

The triangle singularities occur in the box diagram and correspond to essentially the same physical pictures

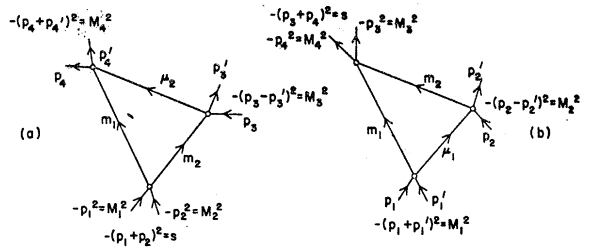

FIG. 6. Two examples where transitions can occur with three internal particles of the box diagram on the mass shell. In case (a), $x>1$, $x_4>1$, $x_3=L^+(x,x_4)<-1$, and the values of y, x_1, and x_2 are irrelevant. In case (b), $x>1$, $x_1>1$, $x_2=L^+(x,x_1)<-1$.

as in the triangle graph. We define[8]

$$x=(s-m_1^2-m_2^2)/2m_1m_2,\ y=(t-\mu_1^2-\mu_2^2)/2\mu_1\mu_2\,, \quad (9a)$$

and

$$\begin{aligned} x_1&=(M_1^2-\mu_1^2-m_1^2)/2\mu_1m_1\,,\\ x_2&=(M_2^2-\mu_1^2-m_2^2)/2\mu_1m_2\,,\\ x_3&=(M_3^2-\mu_2^2-m_2^2)/2\mu_1m_1\,,\\ x_4&=(M_4^2-\mu_2^2-m_1^2)/2\mu_2m_1\,, \end{aligned} \quad (9b)$$

and note from the discussion in Sec. II that the reaction in Fig. 6(a) is possible when $x_4>1$, $x_3<-1$, $x_3+x_4<0$, and $x=L_{34}^-$. Similarly, the situation depicted in Fig. 6(b) can occur when $x_1>1$, $x_2<-1$, $x_1+x_2<0$, and $x=L_{12}^-$. By combining these singularities with the $L_{14}^\pm$ and $L_{23}^\pm$ which likewise exist in the t channel, we obtain all the triangle singularities $L_{12}^\pm$, $L_{34}^\pm$, $L_{14}^\pm$, and $L_{23}^\pm$. Each of these has values of the x_i and x, y which locate them on the physical boundary.

In addition to the $L_{ij}^\pm$, there are of course the normal thresholds $x=1$, $y=1$, $x_i=1$. As discussed in Sec. II, they always lie on the physical boundary.

Finally we must consider the singularities which correspond to all four internal particles on the mass shell. Let us study the requirements for such a reaction to occur. Three possible configurations are shown in Fig. 7, and it is easy to verify that any other can be obtained from one of these by relabeling the vertices (and/or reversing all the velocities).

Let us look at the conditions which allow the process shown in Fig. 7(a). It is convenient for this purpose to think of the transition as occuring in two stages; the first below the dotted line in Fig. 7(a), and the second above this line. We fix the $x_i(x_1,x_4>1\,;\,x_2,x_3<-1)$ and ask what restrictions are imposed on x and y. Consider the first step of this reaction in the coordinate system where m_1 is produced at rest. This is shown in Fig. 8(a), and it is apparent that the possible range of $x(s)$ is determined directly by the allowed velocities of m_2. This velocity is minimum (maximum) when m_2 is emitted backward (forward) relative to μ_1. If m_2 is emitted forward (x maximum), then it necessarily ends up moving away from m_1. If it is ejected backwards (x minimum), it moves toward or away from m_1 depending upon the velocity of μ_1 and the momentum transferred at the second vertex. For $x_1+x_2>0$, it moves away; for $x_1+x_2<0$, it goes toward m_1. In either case, the allowed range of x is[12] $L_{12}^-<x<L_{12}^+$ (see also the Appendix). These results are summarized in Fig. 8.

The part of Fig. 7(a) above the dashed line is essentially the same as that below, if the directions of all velocities are reversed. Accordingly, the possible values of x are given by $L_{34}^-<x<L_{34}^+$. This subprocess is represented in Fig. 8(b). For $x_3+x_4<0$, and x sufficiently near L_{34}^-, m_2 interacts with M_3 when it (m_2) has a component of velocity away from m_1. If $x_3+x_4>0$, or if x is sufficiently close to L_{34}^+, m_2 must have a positive component of its velocity toward m_1.

To put the two parts of Fig. 8 together to form the reaction of Fig. 7(a), it is clear that there must exist a range of x which satisfies both $L_{12}^-<x<L_{12}^+$ and $L_{34}^-<x<L_{34}^+$. Thus, either $L_{34}^-<L_{12}^-<L_{34}^+$ or $L_{12}^-<L_{34}^-<L_{34}^+$. If one of these conditions is fulfilled, there is an interval of x where both stages of Fig. 7(a) are energetically possible. Now let's look at the geometric requirements. For fixed x_i, the value of x determines the angles θ_1 and θ_2 shown in Fig. 8. The realization of Fig. 7(a) therefore depends upon whether m_2, when emitted in the direction given by θ_1, can unleash μ_2 with the required θ_2. This feat can be accomplished if, and only if,

$$\pi-\theta_1<\theta_2\,. \quad (10)$$

If the inequality (10) is satisfied, m_2 can propagate for exactly the right distance to fire μ_2 in the direction determined by θ_2 and hit m_1 "head-on." When $\theta_2=\pi-\theta_1$, the distance traveled by m_2 is zero, and for $\theta_2<\pi-\theta_1$, the two states of Fig. 8 are incompatible.

If $x_1+x_2>0$ and $x_3+x_4>0$, then we see from Fig. 8 (and the above discussion) that both θ_1 and θ_2 lie in the interval $0<\theta_i<\pi/2$. The inequality (10) can not

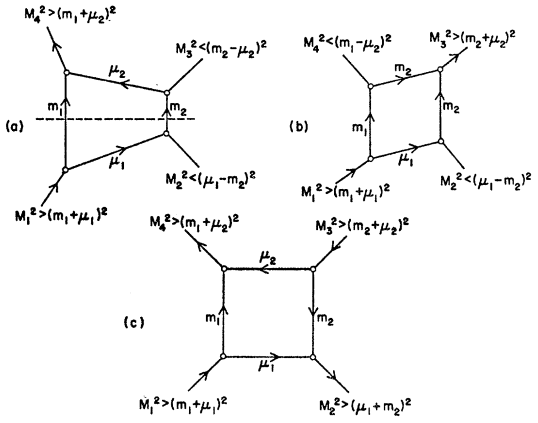

FIG. 7. Three different configurations for transitions with four real internal particles. Any other can be obtained from one of these by relabeling the vertices.

[12] R. F. Peierls, Phys. Rev. Letters 6, 641 (1961).

TABLE I. All the regions of x where the configurations in Fig. 7 can actually occur. When the x_i are adjusted as indicated, the singularity $y_+(x)$ is on the physical boundary if, and only if, x lies in these regions.

Figure	Restrictions on the X_i	Restrictions on the $L_{ij}^{\pm}$	Location of "Box" singularity in x and y
7(a)[a]	$x_1>1$, $x_4>1$, $x_2<-1$, $x_3<-1$, and $x_1+x_2<0$	$1<L_{34}^-<L_{12}^-<L_{34}^+<L_{12}^+$, then $L_{23}^+<L_{14}^+<L_{23}^-<L_{14}^-<-1$; or $1<L_{34}^-<L_{12}^-<L_{12}^+<L_{34}^+$, then $L_{23}^+<L_{14}^+<L_{14}^-<L_{23}^-<-1$	$L_{12}^-<x<x_0<L_{34}^+(L_{12}^+)$ such that $y_+(x_0)=L_{14}^+$; then $L_{14}^+<y=y_+(x)<y_+(L_{12}^-)<L_{23}^-$, or $L_{14}^+<y=y_+(x)<y_+(L_{12}^-)<L_{14}^-$
7(b)[b]	$x_1>1$, $x_3>1x_2<-1$, $x_4<-1$, and $x_1+x_2<0$	$1<L_{34}^-<L_{12}^-<L_{34}^+<L_{12}^+$, then $1<L_{23}^-<L_{14}^-<L_{23}^+<L_{14}^+$	$L_{12}^-<x<x_0<L_{34}^+$, such that $y_+(x_0)=L_{14}^-$; then $L_{14}^-<y=y_+(x)<y_+(L_{12}^-)<L_{23}^+$
		$1<L_{34}^-<L_{12}^-<L_{12}^+<L_{34}^+$, then $1<L_{14}^-<L_{23}^-<L_{23}^+<L_{14}^+$	$L_{12}^-<x<x_0<L_{12}^+$, such that $y_+(x_0)=L_{23}^-$; then $L_{23}^-<y=y_+(x)<y_+(L_{12}^-)<L_{23}^+$
7(c)[b]	all $x_i>1$	$L_{12}^+<L_{34}^+<L_{12}^-<L_{34}^-<-1$, then $L_{14}^+<L_{23}^+<L_{14}^-<L_{23}^-<-1$	$L_{34}^+<x<x_0<L_{12}^-$, such that $y_+(x_0)=L_{23}^+$ then $L_{23}^+<y=y_+(x)<y_+(L_{34}^+)<L_{14}^-$
		$L_{12}^+<L_{34}^+<L_{34}^-<L_{12}^-<-1$, then $L_{23}^+<L_{14}^+<L_{14}^-<L_{23}^-<-1$	$L_{34}^+<x<x_0<L_{34}^-$, such that $y_+(x_0)=L_{14}^+$, then $L_{14}^+<y=y_+(x)<y_+(L_{34}^+)<L_{14}^-$

[a] Two more cases obtained by interchanging $1\leftrightarrow 4$ and $2\leftrightarrow 3$.
[b] Two more cases obtained by interchanging $1\leftrightarrow 3$ and $2\leftrightarrow 4$.

be satisfied. Consider, however, $L_{34}^-<L_{12}^-<L_{34}^+$, and x just larger than L_{12}^-. The angle θ_1 is then barely less than π, and the requirements of (10) can clearly be fulfilled. As x increases from L_{12}^-, θ_1 decreases from π toward zero, but before it gets there x reaches x_0, say, where $\theta_1=\pi-\theta_2$. At this value of x, the distance traversed by m_2 has shrunk to zero, and the corresponding singularity must be on the verge of leaving the physical boundary.

Suppose the x_i and x are adjusted to allow the process of Fig. 7(a). If we compute the value of y which is required, we obtain

$$y=y_+(x)\equiv 1/(x^2-1)\{x(x_1x_3+x_2x_4)+x_1x_4+x_2x_3 +[(x-L_{12}^-)(x-L_{12}^+)(x-L_{34}^-)(x-L_{34}^+)]^{1/2}\}, \quad (11)$$

or expressing x in terms of y,

$$x=x_-(y)\equiv 1/(y^2-1)\{y(x_1x_3+x_2x_4)+x_1x_2+x_3x_4 -[(y-L_{14}^-)(y-L_{14}^+)(y-L_{23}^-)(y-L_{23}^+)]^{1/2}\}. \quad (12)$$

The algebra needed to yield this result is outlined in the Appendix. Equations (11) and (12) describe one of the two "well-known" box-diagram singularities.[6,8] The other, $y=y_-(x)$ or $x=x_+(y)$, is obtained by changing the sign of the square roots in Eqs. (11) and (12). It can similarly be located on the physical boundary by considering the process differing from that in Fig. 7(a) by the interchange of M_2 and M_4. This replacement reverses the roles of x and y.

We can now see how the singularity given by Eqs. (11) or (12) leaves the physical boundary when x increases past the position of x_0 discussed above. At this point, m_2 does not propagate any distance at all, and the configuration of Fig. 7(a) degenerates into that of Fig. 9. Comparing this situation with that shown in Fig. 3, and with the discussion in Sec. II, we conclude that the singularity $y=y_+(x)$, which lies on the physical boundary for $L_{12}^-<x<x_0$, disappears from this limit by moving behind the triangle singularity $y=L_{14}^+$. That is, $y_+(x_0)=L_{14}^+$, or $x_0=x_-(L_{14}^+)$.

The other alternative for the realization of Fig. 7(a), $L_{12}^-<L_{34}^-<L_{12}^+$, can be similarly analyzed. In the part of Table I which refers to Fig. 7(a), we list all the regions where the possibility of this configuration implies a box diagram singularity located on the physical boundary.

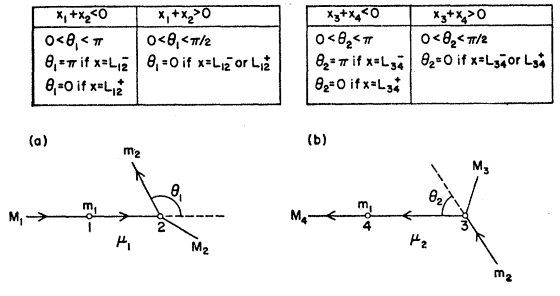

FIG. 8. The two subprocesses divided by the dashed line in Fig. 7(a) are shown separately in the coordinate system where m_1 is produced at rest. The ranges of the angles θ_1 and θ_2 are also given.

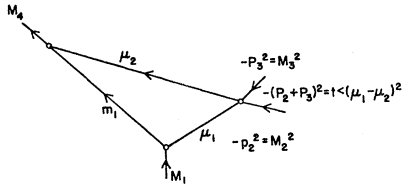

FIG. 9. A picture of the process in Fig. 7(a) when $\theta_2=\pi-\theta_1$, so that m_2 interacts with M_3 as soon as it is created by M_2. The box diagram singularity $y_+(x)$ coincides with the triangle singularity L_{14}^+.

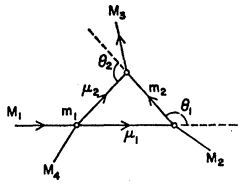

FIG. 10. The process in Fig. 7(b) is portrayed in the coordinate system where m_1 is produced at rest. In contrast to the case of Fig. 7(a), $\theta_2>\pi-\theta_1$ is not a sufficient condition for this reaction to proceed. It is also necessary that m_1 is not required to emit μ_2 before it (m_1) is created by M_1.

The domains where the processes in Figs. 7(b) and 7(c) are possible are also listed in Table I. The arguments leading to these results are similar to those already discussed. For example, consider the s_i and $L_{ij}^{\pm}$ arranged according to the first case of Table I referring to Fig. 7(b). This reaction is portrayed in Fig. 10, and it is readily seen that the angles θ_1 and θ_2 must again satisfy the inequality (10). For x just larger than L_{12}^{-}, θ_1 is barely less than π, and (10) can easily be satisfied. As x increases from L_{12}^{-}, the angle θ_1 decreases, and the velocity of m_2 gets larger. As before, there will exist a point where $\theta_2=\pi-\theta_1$, and if the process has been possible until then, it will not be for larger values of x. This situation is similar to the previous case, and the singularity $y_+(x)$ will disappear from the physical boundary by passing behind L_{14}^{-}. These features characterize the first case for Fig. 7(b) shown in Table I. It is also possible, however, that the point $\theta_1=\pi-\theta_2$ can not be reached. Before this occurs, m_1 may be required to emit μ_2 as soon as it (m_1) is produced by M_1. This is the second alternative in Table I, and one sees that the relevant singularity leaves by ducking under L_{23}^{-}. Similar considerations apply for Fig. 7(c).

B. Mathematical Considerations

Let us now show that the conclusions of part A, for the location of $y_+(x)$, agree with those obtained by analytic continuation of the box diagram amplitude in the external masses.

When $x_i<1$, $x_1+x_2<0$, $x_1+x_4<0$, $x_3+x_4<0$, and $x_2+x_3<0$, a Mandelstam representation is valid for the diagram of Fig. 5.[6,8] Suppressing the dependence upon the $M_i^2(x_i)$, and replacing the variables s and t by x and y, this representation can be written as

$$B(x,y)=\frac{1}{\pi}\int_1^{\infty}\frac{dx'}{x'-x}f(x',y), \tag{13}$$

where

$$f(x',y)=\frac{1}{\pi}\int_{y_+(x')}^{\infty}\frac{dy'}{y'-y}K^{-1/2}(x',y'), \tag{14}$$

and

$$K(x,y)=(x^2-1)(y-y_-(x))(y-y_+(x))$$
$$=(y^2-1)(x-x_+(y))(x-x_-(y)). \tag{15}$$

The $y_{\pm}(x)$ and $x_{\pm}(y)$ are given by Eqs. (11) and (12) and by the discussion immediately following.

The function $f(x',y)$ defined in Eq. (14) has singularities at $x'=\pm1$, $L_{12}^{\pm}$, $L_{34}^{\pm}$ and at $y=y_{\pm}(x')$. The $x'=\pm1$ occur because then the two singularities of $K(x',y)$, $y=y_-(x')$ and $y=y_+(x')$, go to infinity; $x'=1$, of course, yields the normal threshold which is also manifest in Eq. (13); $x'=-1$ is never on the physical boundary as argued in Sec. II. The $L_{ij}^{\pm}$ account for the possibility that the two zeros of $K(x',y)$ can "pinch" the contour in Eq. (14). The $y_+(x')$ is explicit in Eq. (14), and $y_-(x')$ is only singular if it "pinches" the contour against y. This will not occur for any of the continuations which are considered.

Suppose now that y is held fixed in the upper half-plane, and that the x_i are varied, with small, positive imaginary parts, along their real axes to the region x_1, $x_4>1$; x_2, $x_3<-1$. During this continuation, the $L_{ij}^{\pm}$ do not cross[13] the line $x'>1$, and $y_+(x')$, for $x'>1$, does not move into the upper y' plane. We can therefore accomplish this continuation without distorting the x' contour in Eq. (13). For definiteness, we adjust x_2 and x_3 to their final values before increasing x_1 and x_4, and locate the x_i to satisfy $x_1+x_2<0$ and $x_3+x_4<0$. Except for possible reorderings of the $L_{ij}^{\pm}$ along the line $x'>1$, these singularities of $f(x',y)$ then move from their initial to their final values as shown by the dotted lines in Fig. 11(a). Simultaneously, $L_{14}^{\pm}$ and $L_{23}^{\pm}$ assume the positions in the y' plane shown in Fig. 11(b).

We want to show that if x and y approach the physical region from their upper half-planes, then $y=y_+(x)$ is a singularity of $B(x,y)$ in Eq. (13) if, and only if, $L_{12}^{-}<x<x_-(L_{14}^{+})$—that is, if the conditions derived in part A and listed for this case in Table I are satisfied. Consider x' to vary along the integration

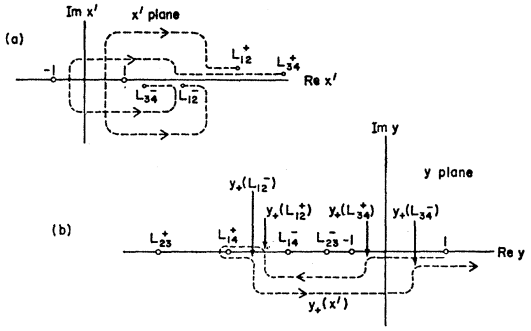

FIG. 11. A typical arrangement of $L_{12}^{\pm}$ and $L_{34}^{\pm}$ in the x_i plane and of $L_{23}^{\pm}$ and $L_{14}^{\pm}$ in the y plane is shown. The dashed lines in (a) indicate how $L_{12}^{\pm}$ and $L_{34}^{\pm}$ move to their final positions when the x_i are continued from $x_i^2<1$ to $x_1>1$, $x_4>1$, $x_2<-1$, $x_3<-1$ with $x_1+x_2<0$ and $x_3+x_4<0$. The dashed lines in (b) indicate how the singularity $y_+(x)$ moves as x' is decreased from $+\infty$ to $+1$ passing under L_{12}^{+} and L_{34}^{+} and over L_{12}^{-} and L_{34}^{-}.

[13] If x_1 and x_4 are continued above $+1$ before x_2 and x_3 are decreased below -1, the L_{12}^{+} and L_{34}^{+} cross the line $x>1$; they return, however, as soon as x_2 and x_3 are decreased below -1.

contour of Eq. (13), moving in from $+\infty$ under L_{34}^{+} and L_{12}^{+} and over L_{12}^{-} and L_{34}^{-} before proceeding to $+1$ [see Fig. 11(a)]. As x' decreases from ∞, $y_+(x')$ decreases from $+1$; it then goes into the lower half-plane for $L_{12}^{+}<x'<L_{34}^{+}$, converges on the real axis when $x'=L_{12}^{+}$, loops L_{14}^{+} at some point x_0 between L_{12}^{-} and L_{12}^{+}, goes into the lower half-plane for $L_{34}^{-}<x'<L_{12}^{-}$, and moves off to $+\infty$ as x' approaches $+1$. This motion is shown by the dotted line in Fig. 11(b).

During this journey, whenever $y_+(x')$ resides in the physical region determined by the value of x', it may introduce a singularity of $B(x,y)$ on the physical boundary. For $B(x,y)$ to be singular when x and y both approach the real axis from above, it is necessary that x, pushing down on the contour of Eq. (13), forces the singularity $y=y_+(x)$ up at y. This means that $dy_+/dx<0$. From the preceding discussion of the motion of $y_+(x')$ [and Fig. 11(b)], we see that this situation only happens in the required interval $L_{12}^{-}<x<x_-(L_{14}^{+})$ so that $L_{14}^{+}<y_+(x)<y_+(L_{12}^{-})$, and also for a portion of the region where both x and $y_+(x)$ lie outside their respective $L_{ij}^{\pm}$. The latter domain never lies within the physical range of variables (see the Appendix).

C. Determination of the Amplitude

We here argue that the box diagram amplitude is determined once Cutkosky's rules are supplemented by the conclusions of part A. Let us, for this purpose, again adjust the x_i to satisfy the conditions which allow the reaction in Fig. 7(a) and fix the $L_{ij}^{\pm}$ to agree with Fig. 11. If the value of y is also stationed along its negative, real axis in the region $L_{14}^{+}<y<y_+(L_{12}^{-})$, then we know from part A that the singularities $x=1$, L_{34}^{-}, L_{12}^{-}, and $x_-(y)$ all lie on the physical boundary, whereas the L_{12}^{+}, L_{34}^{+}, and $x_+(y)$ do not. Proceeding as in Sec. II for the triangle diagram, we employ Cutkosky's rules to calculate the dispersion integrals in x' (fixed y) contributed by the four branch points $x=1$, L_{12}^{-}, L_{34}^{-}, and $x_-(y)$. As before, these contributions can be summed to yield

$$B(x,y)=\frac{1}{\pi^2}\int_1^{\infty}\frac{dx'}{x'-x}\frac{1}{[K(x',y)]^{1/2}}\times\ln\left[\frac{y_+(x')+y_-(x')-2y+2[(y_+(x')-y)(y_-(x')-y)]^{1/2}}{y_+(x')+y_-(x')-2y-2[(y_+(x')-y)(y_-(x')-y)]^{1/2}}\right], \tag{16}$$

where the integration contour runs over the L_{ij}^{-} and $x_-(y)$, but under the L_{ij}^{+} and $x_+(y)$. Equation (16) could also be obtained by performing the integration in Eq. (14).

The amplitude $B(x,y)$ is now determined up to a choice of branch for the logarithm in Eq. (16). To decide this question, we note that if y is increased over $y_+(L_{12}^{-})$ so that it sits in the interval $y_+(L_{12}^{-})<y<L_{14}^{-}$, then $x_-(y)$ decreases, loops clockwise around L_{12}^{-} and comes back. As it returns, it must not be a singularity of the integrand in Eq. (16); if it were, it would introduce a singularity of $B(x,y)$ for a region of y not allowed by the conclusions of part A. Inversely, if y is held fixed in the domain $L_{14}^{+}<y<y_+(L_{12}^{-})$, and x' in the integrand of Eq. (16) is decreased from $x_-(y)$ and looped counter-clockwise around L_{12}^{-}, it must return to $x_-(y)$ when the logarithm of (16) is on its principal branch. The branch of the integrand in Eq. (16) is thereby determined. For x' larger than all the $L_{ij}^{\pm}$, it assumes its principal value.

IV. CONCLUDING REMARKS

We have seen two special cases how kinematic and geometric considerations may be employed to fix the proper Riemann sheets for all the singularities appearing in these amplitudes. In fact, the method used did not seem to exploit all the information which these considerations offered. For example, in our determination of the amplitude for the triangle graph, we did not explicitly use the fact that L_{23}^{+} must show up on the physical boundary, $x_1<-1$, when x_2 and x_3 are both increased above $+1$. If the techniques employed here to locate singularities are found useful in more general applications, it would probably not always be possible to fix them all simultaneously. That is, it would presumably be necessary to put one (or a few) after the other of these singularities on the physical boundaries of the amplitude, thereby locating them in turn. To actually carry out this program, some domain of analyticity would be required through which the continuation from one physical boundary to the next could be accomplished. For the amplitudes considered here, this domain is the product of the upper half planes of the M_i^2 (and s and t).

ACKNOWLEDGMENTS

The author is grateful to Professor Christian Fronsdal for numerous stimulating discussions. He also wishes to thank the Physics Division of the Aspen Institute of Humanistic Studies, Aspen, Colorado, for its hospitality during the Summer of 1963.

APPENDIX

We here outline the steps required to obtain Eq. (11). We consider the process in Fig. 7(a), and its two parts in Fig. 8(a), (b), in the c.m. system of M_3 and M_4 or m_1 and m_2. We call ϕ_1 the angle between the incoming M_1 and the outgoing m_1 for the reaction of Fig. 8(a), and define ϕ_2 to be the angle between m_1 and M_4 in the process of Fig. 8(b). One can readily obtain

$$\cos\phi_1=\frac{\alpha_1}{\beta_1}=\frac{s^2-s(M_1^2+M_2^2+m_1^2+m_2^2-2\mu_1^2)+(M_1^2-M_2^2)(m_1^2-m_2^2)}{[\Delta(s,M_1^2,M_2^2)\Delta(s,m_1^2,m_2^2)]^{1/2}}, \tag{A1}$$

$$\cos\phi_2=\frac{\alpha_2}{\beta_2}=\frac{s^2-s(M_3^2+M_4^2+m_1^2+m_2^2-2\mu_2^2)+(M_4^2-M_3^2)(m_1^2-m_2^2)}{[\Delta(s,M_3^2,M_4^2)\Delta(s,m_1^2,m_2^2)]^{1/2}}, \tag{A2}$$

where the symbols are defined in Fig. 5 and Eq. (1). If the two parts in Fig. 8 are now put together to form the transition in Fig. 7(a), and if ϕ is defined to be the angle between M_1 and M_4, then

$$\cos\phi=\cos(\phi_1+\phi_2)=\cos\phi_1\cos\phi_2-[(1-\cos^2\phi_1)(1-\cos^2\phi_2)]^{1/2}. \tag{A3}$$

We now look at Fig. 5, and express t in terms of s, $\cos\phi$, and the M_i^2,

$$t=(1/2s)\{-s^2+s(M_1^2+M_2^2+M_3^2+M_4^3)-(M_1^2-M_2^2)(M_4^2-M_3^2)+\cos\phi[\Delta(s,M_1^2,M_2^2)\Delta(s,M_3^2,M_4^2)]^{1/2}\}. \tag{A4}$$

Substituting (A1)–(A3) into (A4) and replacing s, t and the M_i^2 by x, y, and the x_i according to Eqs. (9a), (9b), there results Eq. (11).

The remark at the end of part B, Sec. III can also be easily verified. For x outside both the intervals $L_{12}^-<x<L_{12}^+$ and $L_{23}^-<x<L_{34}^+$, then $\cos\phi_1$ and $\cos\phi_2$ defined in (A1) and (A2) are both larger than unity in magnitude. Therefore, by (A3), so is $\cos\phi$, and y_+ does not lie in the physical region $|\cos\phi|<1$.

PHYSICAL REVIEW VOLUME 135, NUMBER 6B 21 SEPTEMBER 1964

Depolarization of Spin-½ Particles by Electromagnetic Scatterings

C. K. IDDINGS* AND G. L. SHAW*
Institute of Theoretical Physics, Department of Physics, Stanford University, Stanford, California
AND
Y. S. TSAI†
Stanford Linear Accelerator Center, Stanford University, Stanford, California
(Received 27 April 1964)

A study is made of the depolarization of polarized, relativistic fermions (spin ½) passing through matter. The final polarization of the projectile shows two features, (i) a rotation of the polarization vector so that it does not have the same direction as the initial polarization with respect to the initial or final momenta: *rotation*; (ii) an unpolarized component so that the magnitude of the polarization has diminished: *shrinkage*. We consider the scattering of the incident polarized fermion off unpolarized target electrons and nuclei to lowest order in α. Whereas to this order no polarization can be produced, i.e., the magnitude of the polarization vector cannot increase, the magnitude of the spin vector can decrease if the target has spin. General formulas are presented for the spin-½ particles scattered electromagnetically from an unpolarized target with arbitrary spin in terms of form factors. Numerical results are presented for processes (i) and (ii) in the cases of positrons and muons scattered by unpolarized electrons. Process (ii) is proportional to t^2 (for small momentum transfer t). If one expands the expressions for the polarization phenomena keeping only the linear term in t, then the shrinkage (ii) vanishes and the rotation effects (i) all reduce to those for the pure Coulomb scattering case. (As is well-known the depolarization due to Coulomb scattering is negligible for small-angle scattering.) However, if one is concerned with particles scattered into a sizeable solid angle, then (a) the rotation effects in, e.g., positron-electron scattering become enormously larger than that given by Coulomb scattering; (b) they become strongly dependent on the relative orientation of the incident polarization vector: much larger rotations occur for transversely polarized beams; (c) one cannot omit the contribution from the annihilation diagram compared to that from the direct one-photon exchange; (d) and *most important* the depolarization due to shrinkage is *comparable* to the rotational effects. In multiple scattering, the shrinkage is a cumulative effect whereas the rotational contribution to depolarization is a random walk process.

I. INTRODUCTION

DETAILED knowledge of the depolarization of polarized, relativistic fermions (spin ½) passing through matter is of current interest. Our theoretical studies (which neglect bremsstrahlung, see Ref. 21) do not explain the large depolarizations found in the experiments of Dick *et al.*[1,2] However, our results show a

* Supported in part by the U. S. Air Force through Air Force Office of Scientific Research Grant AF-AFOSR-62-452.
† Supported by U. S. Atomic Energy Commission.

[1] L. Dick, L. Feuvrais, and M. Spighel, Phys. Letters 7, 150 (1963); S. Bloom, L. A. Dick, L. Feuvrais, G. R. Henry, P. C. Macq, and M. Spighel, *ibid.* 8, 87 (1964); L. Dick, L. Feuvrais, L. DiLella, and M. Spighel, *ibid.* 10, 236 (1964).

[2] However, we do get agreement with the small μ depolarization observed experimentally. Polarized muons suffer negligible depolarization in slowing down from ~70 to ~10 MeV in any type of moderator [D. D. Yovanovitch (private communication)].